

# Physics Potential of the $\gamma = 100, 100$ Beta Beam

Mauro Mezzetto <sup>a</sup>

<sup>a</sup>Istituto Nazionale Fisica Nucleare, Sezione di Padova. Via Marzolo 8, 35100 Padova, Italy.

The physics potential of a Beta Beam fired from CERN to a 440 kton water Cerenkov detector at a distance of 130 Km is computed.

## 1. Introduction

Beta Beam ( $\beta\text{B}$ ) [1] performances have been computed for  $\gamma(^6\text{He}) = 66$  [2], 100 [3] [4] [5], 150 [5], 200 [7], 350 [5], 500 [6] [7], 1000 [7], 2000 [6], 2488 [8]. A review can be found in [9], physics potential of low gamma  $\beta\text{B}$  has been studied in [10]. Performances of  $\beta\text{B}$  with  $\gamma > 150$  are extremely promising but rather speculative, because they are not based on an existing accelerator complex nor on a robust estimation of the ion decay rates. For a CERN based Beta Beam, fluxes have been estimated in [11], and the physics potential for a beam fired to a 440 kton water Cerenkov detector [12] hosted under the Frejus, at 130 km from CERN, has been firstly computed in [2]. So far the Frejus site [13] is the only realistic candidate at a suitable baseline for a CERN based  $\beta\text{B}$  with  $\gamma \leq 150$ .

This work updates and consolidates performances computed in [3] for a  $\beta\text{B}$  where both  $^6\text{He}$  and  $^{18}\text{Ne}$  ions have  $\gamma = 100$  ( $\beta\text{B}100$ ), the optimal setup for a 130 km distance. In particular signal efficiency, background estimation, energy binning will be revised and all the sensitivities will be computed using the open source program Globes [14], allowing for an estimation of performances in presence of degeneracies. Finally the Beta Beam performances will be computed as function of the duty cycle.

## 2. Signal and backgrounds

### 2.1. Signal efficiency

Signal events in  $\beta\text{B}$ ,  $\nu_\mu$  charged current (CC) events, are selected with standard SuperKamiokande particle identification algorithms. The muon identification is reinforced

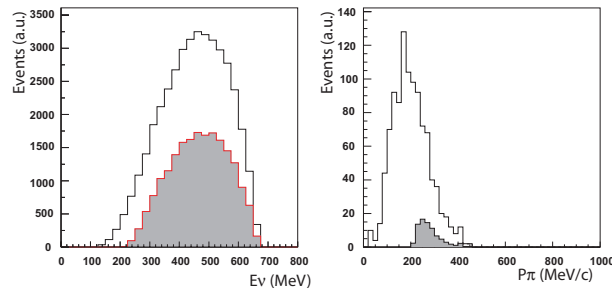


Figure 1. Left: Event reduction for  $^{18}\text{Ne}$  oscillated events (left) and pion background,  $\pi^+ + \pi^-$  (right).

by asking for the detection of the Michel decay electron. Data reduction is shown in fig. 1 for  $^{18}\text{Ne}$  events and detailed in tab. 1.

### 2.2. Energy binning

As pointed out in reference [5], it is necessary to use a migration matrix to properly handle the Fermi motion smearing in the  $\beta\text{B}100$  energy range. The matrices, computed with Nuance [15], have 25 true energy bins and 5 reconstructed energy bins in the energy range  $0 < E_\nu < 1$  GeV, see fig. 2. The migration matrix approximation has a visible effect in the Leptonic CP Violation discovery potential, as discussed in section 3.

### 2.3. Atmospheric neutrino backgrounds

Atmospheric neutrino can constitute an important source of backgrounds [1]. They can be suppressed only by keeping a very short duty cycle, and this in turn is one of the most challenging bounds on the design of the Beta Beam complex.

To compute the rate of this background, the total integrated rate of atmospheric  $\nu_e$  in SK, in the energy range of  $\beta\text{B}100$ , is considered. This rate is scaled to the 440 kton fiducial mass and corrected for the difference of atmospheric neutrino fluxes between Kamioka and Frejus [16]. The direction

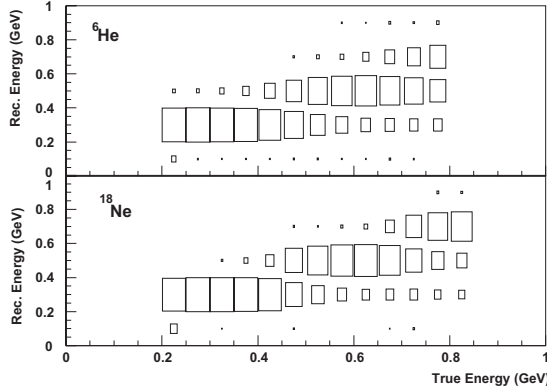


Figure 2. Migration matrices for  ${}^6\text{He}$  (upper plot) and  ${}^{18}\text{Ne}$  (lower plot).

of the incident neutrino at 400 MeV, according to Nuance, can be reconstructed with a  $\sim 0.25$  radians resolution. A  $2\sigma$  cut around the CERN-Frejus direction is then applied. Finally the efficiency curves of section 2.1 are applied to the remaining events. Assuming 8 bunches 6.25 ns long in the 7 km long decay ring, the duty cycle is  $2.2 \cdot 10^{-3}$ . Atmospheric neutrino backgrounds sum up to 13 background events per ion specie in a 4400 kton-year exposure ( $10^7$  s/year).

In the following, sensitivities are computed with this background, the effect of a higher duty cycle is discussed in session 4.

#### 2.4. Charged pions background

Charged pions generated in NC events (or in NC-like events where the leading muon goes undetected) are the main source of background for the experiment. To compute this background inclusive NC and CC events have been generated with the  $\beta\text{B100}$  spectrum. Events have been selected where the only visible track is a charged pion above the Cerenkov threshold. Particle identification efficiencies have been applied to those particles. With Geant 3.21 the probability for a pion to survive in water until its decay have been computed<sup>1</sup>. This probability is different for positive and negative pions, these latter having a higher probability to be absorbed before decaying. The surviving events are backgrounds and the reconstructed neutrino energy is computed mis-identifying these pions as muons. Event rates are reported in tab. 1. These background rates

<sup>1</sup>cross-checked with a Fluka 2003 simulation [17]

Table 1

Events in a 4400 kton-year exposure.  $\nu_\mu$  ( $\bar{\nu}_\mu$ ) CC events are computed assuming full oscillation, pion backgrounds are computed from  $\nu_e$  ( $\bar{\nu}_e$ ) CC+NC events.

	Ne18			He6		
	$\nu_\mu$ CC	$\pi^+$	$\pi^-$	$\bar{\nu}_\mu$ CC	$\pi^+$	$\pi^-$
in	139181	863	561	107571	952	819
pid	105923	209	123	83419	242	170
dcy	67888	103	6	67727	117	7

are significantly smaller from what quoted in [3], where pion decays were computed with the same probabilities of the muons.

#### 3. Sensitivities

Sensitivity to  $\theta_{13}$  is by definition the performance of the experiment in absence of signal. It has been computed for 10 years running time ( $5 {}^6\text{He} + 5 {}^{18}\text{Ne}$ ) with  $5.8 \cdot 10^{18}$  useful  ${}^6\text{He}$  decays/year and  $2.2 \cdot 10^{18}$  useful  ${}^{18}\text{Ne}$  decays/year. Appearance and disappearance channels have been combined together. Input values are  $\theta_{23} = \pi/4$ ,  $\Delta m_{23}^2 = 2.5 \cdot 10^{-3}$  eV $^2$ ,  $\sin^2 \theta_{12} = 0.315$ ,  $\Delta m_{12}^2 = 7.9 \cdot 10^{-5}$  eV $^2$ ,  $\text{sign}(\Delta m_{23}^2) = +1$ . Parameter errors have been fixed to the T2K sensitivities for the atmospheric parameters [18] and to the present values of the solar parameters:  $\theta_{23} = 5\%$ ,  $\Delta m_{23}^2 = 4\%$ ,  $\theta_{12} = 10\%$ ,  $\Delta m_{12}^2 = 4\%$ . The systematic errors for signal and backgrounds has been fixed to 2%.

The sensitivity curve, fig. 3, is a 6 parameters fit minimized over the solar and the atmospheric parameters and projected over  $\theta_{13}$ . Degeneracies induced by the unknown values of  $\text{sign}(\Delta m_{23}^2)$  and  $\theta_{23}$  are not accounted for.

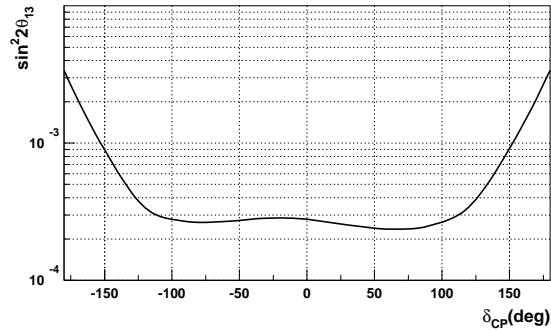


Figure 3.  $\theta_{13}$  sensitivity at 90% CL ( $\Delta\chi^2 > 4.61$ ) as function of  $\delta_{CP}$  (see text).

In case of signal it is important to quantitatively assess the discovery potential for leptonic CP violation (LCPV). It is computed at  $3\sigma$  ( $\Delta\chi^2 = 9.0$ ) taking into account all the parameter errors and all the possible degeneracies. As common practice in literature  $\theta_{23} = 40^\circ$  has been used, to leave room for the octant ( $\pi/4 - \theta_{23}$ ) degeneracy. In fig. 4 discovery potential is computed under 4 different hypotheses of the true parameters, normal:  $\text{sign}(\Delta m_{23}^2) = 1$ ,  $\theta_{23} < \pi/4$ ; sign:  $\text{sign}(\Delta m_{23}^2) = -1$ ,  $\theta_{23} < \pi/4$ ; octant:  $\text{sign}(\Delta m_{23}^2) = 1$ ,  $\theta_{23} > \pi/4$ ; mixed:  $\text{sign}(\Delta m_{23}^2) = -1$ ,  $\theta_{23} > \pi/4$ . Each of these 4 true values combinations has been fitted with the 4 possible fit combinations of  $\text{sign}(\Delta m_{23}^2)$  and  $\theta_{23}$ . Also shown are the LCPV discovery potentials neglecting the degenerate solutions. Effect of degeneracies are sometimes visible for high values of  $\theta_{13}$ , precisely the region where they can be re-

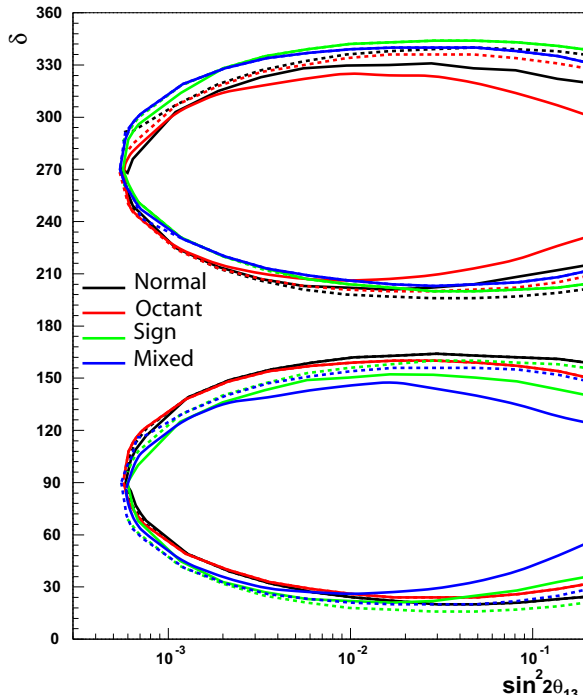


Figure 4. LCPV discovery potential at  $3\sigma(\Delta\chi^2 > 9.0)$  computed for the 4 different options about the true values of  $\text{sign}(\Delta m_{23}^2)$  and  $\theta_{23}$  (see text). Dotted curves are computed neglecting the effects of the clone solutions.

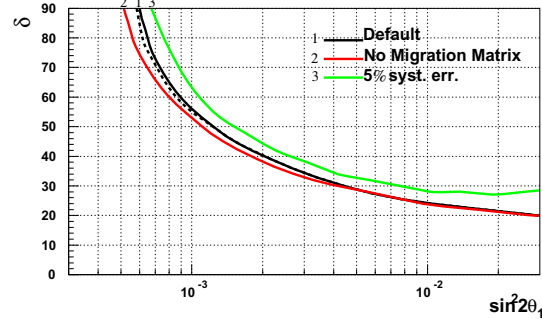


Figure 5. LCPV discovery potential at  $3\sigma(\Delta\chi^2 > 9.0)$ , under three different options of the input parameters (see text) and computed without the degenerate solutions (dotted line).

duced by a combined analysis with atmospheric neutrinos [19].

Several effects play significant roles in the final LCPV discovery potential, as gaussian approximation for the energy binning or systematic errors bigger than 2%, as shown in fig. 5.

#### 4. Duty cycle

A critical parameter in designing the Beta Beam complex is the duty cycle. Due to the available longitudinal acceptance in the decay ring,  $\beta B$  fluxes can only be increased by increasing the number of bunches in the decay ring [20]. An extremely short duty cycle, aimed to keep the atmospheric background close to zero, was the choice for the  $\gamma = 66 \beta B$  [2], where the experimental backgrounds were close to zero. For the  $\gamma = 100$  option, a modest rate of atmospheric neutrino backgrounds is tolerable. To assess the highest possible duty cycle for  $\beta B 100$ , LCPV performances have been computed (neglecting degeneracies) by varying the duty cycle under two hypotheses: the overall fluxes remain constant or the overall fluxes rise as function of the duty cycle as discussed in [20] (fig. 6).

Fig. 7 right, shows performances at constant fluxes. The degradation of performances is evident at the smaller values of  $\theta_{13}$ , where the background level is the dominant factor, while at higher values of  $\theta_{13}$  the performances are rather stable. The left plot of fig. 7 shows performances computed with the flux-duty cycle relationship of fig. 6. Here the nominal fluxes have been assumed

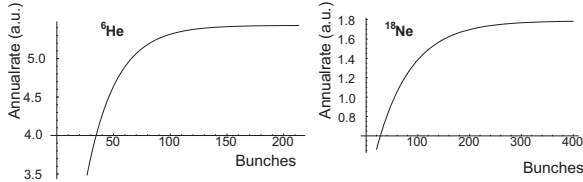


Figure 6. Ion decay rates (a.u.) as function of the duty cycle for  ${}^6\text{He}$  (left) and  ${}^{18}\text{Ne}$  (right). Taken from reference [20].

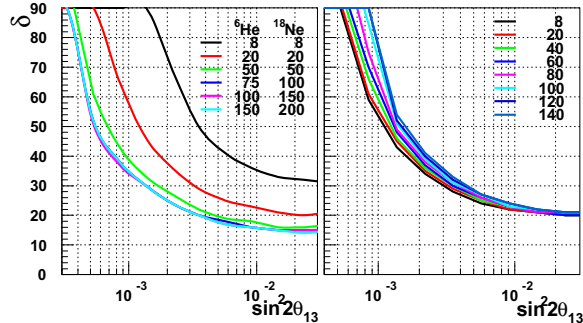


Figure 7. LCPV discovery potential for different values of the number of ion bunches circulating in the decay ring computed following the curves of fig. 6 (left) or keeping constant the ion decay rates (right).

for 20 bunches in the decay ring both for  ${}^6\text{He}$  and  ${}^{18}\text{Ne}$  ions. This assumption is more optimistic of what quoted in [20], the purpose of this plot is not to display performances of  $\beta\text{B100}$  but to show how performances scale as function of the duty cycle. Discovery potential increases up the point where a flux saturation occurs, roughly for 75  ${}^6\text{He}$  bunches and for 150  ${}^{18}\text{Ne}$  bunches. This latter plot shows that the high intensity frontier for the Beta Beams is as promising as the high gamma scenarios.

## 5. Conclusions

The Beta Beam design study for the baseline CERN option is running. It will provide the final estimation of neutrino rates and possible pathways to increase the performances. The physics potential, as can be predicted today, shows that it is worth the effort.

I'm very grateful to J.E. Campagne, P. Huber, M. Lindroos, M. Maltoni and T. Schwetz for the

many illuminating discussions during the preparation of these studies.

## REFERENCES

1. P. Zucchelli, Phys. Lett. B **532** (2002) 166.
2. M. Mezzetto, J.Phys.G29:1781-1784, 2003; [hep-ex/0302007]. J. Bouchez, M. Lindroos and M. Mezzetto, AIP conference proceedings, Vol. 721, 37-47, 2003. [hep-ex/0310059].
3. M. Mezzetto, Nucl. Phys. Proc. Suppl. **149** (2005) 179.
4. A. Donini et al., Nucl. Phys. B **710** (2005) 402 [arXiv:hep-ph/0406132].
5. J. Burguet-Castell et al., arXiv:hep-ph/0503021.
6. J. Burguet-Castell et al., Nucl. Phys. B **695** (2004) 217 [arXiv:hep-ph/0312068].
7. P. Huber et al., arXiv:hep-ph/0506237.
8. F. Terranova et al., Eur. Phys. J. C **38** (2004) 69 [arXiv:hep-ph/0405081].
9. M. Mezzetto, Nucl. Phys. Proc. Suppl. **143** (2005) 309 [arXiv:hep-ex/0410083].
10. C. Volpe, J. Phys. G **30** (2004) L1 [arXiv:hep-ph/0303222].
11. B. Autin et al., physics/0306106. M. Benedikt, S. Hancock and M. Lindroos, Proceedings of EPAC, 2004, <http://accelconf.web.cern.ch/AccelConf/e04>. M. Lindroos, proceedings of this conference.
12. UNO Collaboration, hep-ex/0005046.
13. L. Mosca, Nucl. Phys. Proc. Suppl. **138** (2005) 203.
14. P. Huber, M. Lindner and W. Winter, Comput. Phys. Commun. **167** (2005) 195 [arXiv:hep-ph/0407333].
15. D. Casper, Nucl. Phys. Proc. Suppl. **112** (2002) 161 [arXiv:hep-ph/0208030].
16. G. Barr, T. K. Gaisser and T. Stanev, Phys. Rev. D **39** (1989) 3532.
17. J.E. Campagne, private communication.
18. Y. Itow et al., hep-ex/0106019.
19. P. Huber, M. Maltoni and T. Schwetz, Phys. Rev. D **71** (2005) 053006 [arXiv:hep-ph/0501037].
20. M. Lindroos, EURISOL DS/TASK12/TN-05-02. M. Benedikt, A. Fabich, S. Hancock and M. Lindroos, proceedings of this conference.